




Simulation software of the JUNO experiment

Tao Lin¹, Yuxiang Hu^{1,2}, Miao Yu³, Haosen Zhang^{1,2}, Simon Charles Blyth¹, Yaoguang Wang¹, Haoqi Lu¹, Cecile Jollet⁴, João Pedro Athayde Marcondes de André⁵, Ziyang Deng^{1,a} , Guofu Cao^{1,2,6,b}, Fengpeng An⁷, Pietro Chimenti⁸, Xiao Fang^{1,12}, Yuhang Guo⁹, Wenhao Huang¹⁰, Xingtao Huang¹⁰, Rui Li¹¹, Teng Li¹⁰, Weidong Li¹, Xinying Li^{1,13}, Yankai Liu⁹, Anselmo Mereaglia⁴, Zhen Qian⁷, Yuhan Ren^{1,2}, Akira Takenaka¹¹, Liangjian Wen¹, Jilei Xu¹, Zhengyun You⁷, Feiyang Zhang¹¹, Yan Zhang^{1,14}, Yumei Zhang⁷, Jiang Zhu⁷, Jiaheng Zou¹

¹ Institute of High Energy Physics, Beijing 100049, China

² University of Chinese Academy of Sciences, Beijing 100049, China

³ Wuhan University, Wuhan 430072, China

⁴ University of Bordeaux, CNRS, LP2i, Bordeaux, France

⁵ Institut Pluridisciplinaire Hubert Curien, Université de Strasbourg, Strasbourg, France

⁶ State Key Laboratory of Particle Detection and Electronics, Beijing 100049, China

⁷ Sun Yat-Sen University, Guangzhou 510275, China

⁸ Universidade Estadual de Londrina, Londrina, Brazil

⁹ Xi'an Jiaotong University, Xi'an 710049, China

¹⁰ Shandong University, Qingdao 266237, China

¹¹ Shanghai Jiao Tong University, Shanghai 200240, China

¹² Present address: Chengdu Documentation and Information Center, Chinese Academy of Sciences, Chengdu, China

¹³ Present address: Neusoft Medical Systems Co., Ltd., Shenyang, China

¹⁴ Present address: China Telecom Corporation Limited, Beijing, China

Received: 21 December 2022 / Accepted: 14 April 2023 / Published online: 9 May 2023

© The Author(s) 2023

Abstract The Jiangmen Underground Neutrino Observatory (JUNO) is a multi-purpose experiment, under construction in southeast China, that is designed to determine the neutrino mass ordering and precisely measure neutrino oscillation parameters. Monte Carlo simulation plays an important role for JUNO detector design, detector commissioning, offline data processing, and physics processing. The JUNO experiment has the world's largest liquid scintillator detector instrumented with many thousands of PMTs. The broad energy range of interest, long lifetime, and the large scale present data processing challenges across all areas. This paper describes the JUNO simulation software, highlighting the challenges of JUNO simulation and solutions to meet these challenges, including such issues as support for time-correlated analysis, event mixing, event correlation and handling the simulation of many millions of optical photons.

1 Introduction

The JUNO experiment (Jiangmen Underground Neutrino Observatory) [1,2] is a multi-purpose experiment designed to determine the neutrino mass ordering, precisely measure neutrino oscillation parameters, and probe the fundamental properties of neutrinos by detection of solar neutrinos, galactic core-collapse supernova neutrinos, atmospheric neutrinos, and geo-neutrinos. JUNO will also implement a dedicated multi-messenger (MM) trigger system maximizing its potential as a neutrino telescope by providing sensitivity to low-energy events. In addition, JUNO will provide an excellent environment for nucleon decay searches. JUNO is currently under construction near the city of Jiangmen in southern China, at a distance of 53 km from the Yangjiang and Taishan nuclear power plants, in an underground site with an overburden of ~ 650 m (1800 m.w.e.). Detector commissioning is expected to start in 2023.

The JUNO central detector (CD) is composed of a spherical acrylic volume containing 20,000 tonnes of the liquid scintillator (LS), instrumented with 17,612 20-in. photomultiplier tubes (LPMT) and 25,600 3-in. photomultiplier tubes

^a e-mail: dengzy@ihep.ac.cn (corresponding author)

^b e-mail: caogf@ihep.ac.cn

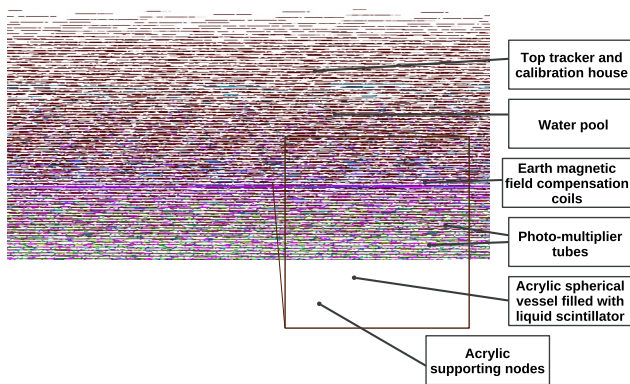


Fig. 1 Schematic of the JUNO detector

(SPMT) with photocathode coverage of 75% and 3%, respectively. The central detector is submerged in a water pool (WP) which is instrumented with 2400 LPMTs providing detection of Cerenkov light from muons and shielding the LS from naturally occurring radioactivity of the surrounding rock. Precise muon track measurements are also provided by the top tracker (TT) detector mounted above the water pool. A schematic view of the detector is presented in Fig. 1 and further details are outlined in prior publications [2,3].

Simulation software is an essential part of the JUNO experiment, providing a flexible and consistent interface to perform simulation studies across a broad physics program. The JUNO simulation software is based on the Geant4 [4–6] toolkit and the SNiPER framework (Software for Non-collider Physics Experiment) [7], which is an experiment independent open-source project with sources available from github [8]. The software has been successfully used to perform massive Monte Carlo production at both local computing resources and distributed computing resources. The MC samples produced have been successfully used for the final selection and optimization of the detector design scheme and have been vital for the development of improved vertex, energy and track reconstruction algorithms. In addition they have enabled definition of the calibration strategy, provided evaluations of natural radioactivity background requirements, and facilitated development of online event classification algorithms, and assisted many physics studies [9–16]. In the past the primary focus of liquid scintillator neutrino experiments was the detection of low energy events, typically below tens of MeV. However for JUNO a much broader energy range is possible from tens of keV up to the level of GeV. The broad energy range and the scale of the JUNO detector with the world's largest scintillator volume present data processing challenges across all areas. This paper addresses the simulation challenges and describes the detailed simulation software implementation in JUNO.

2 Requirements and challenges of JUNO simulation

The simulation software aims to achieve a precise reproduction of experimental data across a broad range of physics analyses in JUNO and is expected to have a software lifetime exceeding 30 years. Attaining this goal requires a longterm commitment to ongoing development that strives to continually improve accuracy, reliability, usability, efficiency, maintainability, and portability. Important simulation challenges for this ongoing work are highlighted below.

- The rich physics program in JUNO leads to the large number of event generators that are essential for the simulation. These generators are implemented with various programming languages and differing output formats. A unified and flexible generator interface is essential to integrate the diverse variety of generators within the JUNO simulation in a cost-effective manner. Various generation tools are also required, for example generating events in given volumes, materials or positions within the detector. In addition, the simulation software should also support the dynamical deployment of calibration sources and the corresponding support structures in the simulation. The proposed solutions are discussed in Sect. 4.
- The simulation requires a large number, of input parameters for the construction of detector geometries and various properties of the simulation including models of the LS, PMT and electronics. Some of these parameters are used by other offline data processing stages in addition to the simulation. Consistency of the parameters across the different stages must be guaranteed. During Monte Carlo tuning, it is also important to be able to vary parameters in a straightforward and flexible way. The parameter management and access strategy is described in Sects. 5.2 and 5.3.
- Mixing simulation events from various sources allows an imitation of real data to be created. However, due to the importance of time correlation and long-time scales for some event types, it is challenging for mixing implementations to fit within memory budgets. For example, inverse beta decays (IBD) yield a positron which can form a prompt readout and a neutron which can form a delayed readout from neutron capture with the average time interval of about 200 μ s. Other decays of radioactive isotopes arising from muons or U/Th decay chains, can yield multiple products with time intervals of milliseconds or even longer. A further consideration is that mixing needs to be done prior to the electronics simulation (at hit level) in order to correctly treat multiple events falling within the readout window (pile-up). As loading all events relevant to long time intervals into memory at once would be prohibitively expensive a novel so-called “pull” technique is developed to implement the mixing

in a much more memory-efficient manner. This method is introduced in Sect. 6.

- Monte Carlo truth information is critical for multiple purposes during data processing and analysis, including algorithm development, understanding detector response, estimating errors, and calculating efficiency in the reconstruction and physics analysis. Providing straightforward access to truth information is extremely useful in many situations. However, after event mixing, a physical process such as IBD could be recorded into multiple readout events. Conversely, one readout event may have contributions from multiple physical events. These complications make it non-trivial to provide full details of the relationship between truth information and the readout events. The proposed solution is presented in Sect. 7.
- The simulation of high energy events within JUNO is important to estimate backgrounds induced by cosmic muons and also for the studies of atmospheric neutrinos and nucleon decays. High energy events can yield huge numbers of optical photons in the LS, for example, tens of millions of photons can be generated from a cosmic muon with a typical energy of 200 GeV crossing the CD. It is challenging to handle the optical photon simulation at this scale within affordable computing resources. We propose several methods to address this issue, including the fast parameterization simulation and the GPU-based full optical photon simulation. They are extensively discussed in Sect. 8.

3 Simulation software architecture

The simulation software is one of the key modules in the JUNO offline software [17]. It depends on the SNIper framework and several other external libraries including Geant4, CLHEP [18], Boost [19] and ROOT [20]. The current versions used are Geant4 10.4.p02 and ROOT 6.24 with upgrades foreseen.

SNIper is designed and developed with Object-Oriented technology and bi-language of C++ and Python. SNIper has many innovations in the management of correlated events by introducing an event buffer mechanism, multi-task processing controlling, and fewer dependencies on third-party software and tools. SNIper also reserves the interfaces to the implementation of multi-threading computing. All modules in the offline software are defined as dynamically loadable elements (DLE) in SNIper, which can be loaded and executed dynamically at run time. The modules to load are configured with Python using interfaces provided by SNIper. The DLEs provide flexible workflow control and memory management.

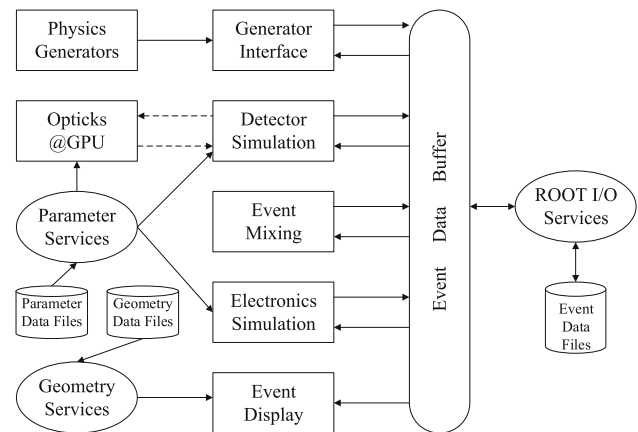


Fig. 2 Architecture of the JUNO simulation software

SNIper roles distinguish the modules into algorithms, services, tasks, and tools. These roles are similar to those of the Gaudi framework [21]. Algorithms are called once per event during the event loop, they create data objects and process data objects in the memory. Services provide common functionalities, like accessing detector geometry information, and provides access to other parts of the framework. A task is a lightweight application manager that orchestrates DLEs and controls the event loop. A SNIper application always starts from a task. The tool is a lightweight routine that enables sharing of a specific functionality between algorithms. In addition to module control, SNIper also provides in-memory data buffer management, job configuration with variable customization, logging information with various output levels, and incident handlers following the Gaudi approach.

The architecture of simulation software is shown in Fig. 2. It consists of four SNIper algorithms of generator interface, detector simulation, event mixing and electronics simulation, a few SNIper services for parameter access, and data I/O management. And it also includes several components that are not strongly coupled or independent with the SNIper framework, such as physics generators, event display, and Opticks [22]. The algorithms are independent of each other. They first read the input data from the event data buffer if necessary, then write the output data back to the buffer after the processing. The buffer data objects are persisted via the ROOT I/O service [23]. The parameter services and geometry services [24, 25] provide requested parameters, and geometry information to other components in the simulation software. Opticks is an open-source package providing GPU-accelerated optical photon simulation that is integrated with the detector simulation. Two event display applications [26, 27] are also developed for debugging, validation, and public outreach. Further details on these components are presented in the following sections.

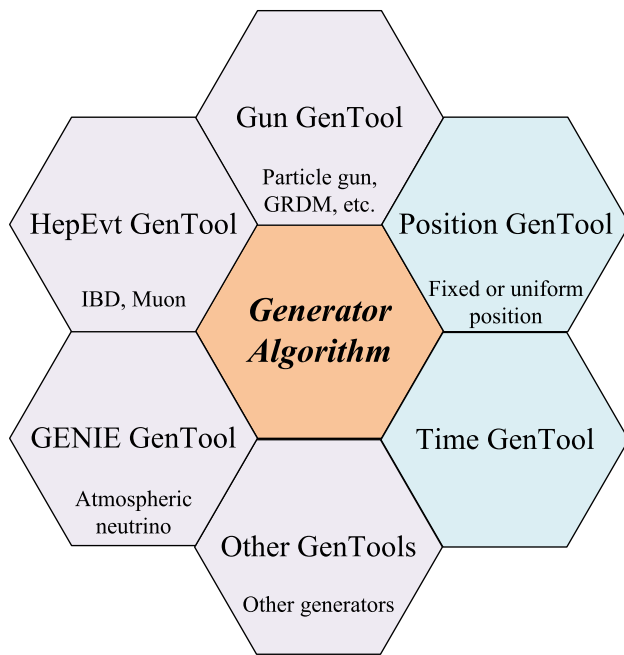


Fig. 3 Overview of physics generator software

4 Physics generators

A variety of physics generators has been developed or integrated with the JUNO offline software system to meet the needs of a broad physics program. The physics generators include generators for cosmic muons, reactor neutrinos, atmospheric neutrinos, solar neutrinos, geo-neutrinos, supernova burst neutrinos, DSNB (Diffuse supernova neutrino background), natural radioactivities, and calibration sources. Most are implemented as standalone packages with differing output formats. A modular physics generator interface is developed, as a SNIper algorithm, to unify the generation of primary particles from various generators. The software design is illustrated in Fig. 3. In the design, the generator algorithm manages a sequence of SNIper tools. The HepMC event record [28] is used as the intermediate data object between the generator algorithm and the generator tools. A *GenEvent* object in HepMC represents a physical event, containing any number of vertex objects named *GenVertex*; each *GenVertex* represents an interaction point with the generated final state particles represented by *GenParticle* objects. The generator algorithm invokes the list of generator tools in sequence to build the HepMC objects. The HepMC objects are subsequently converted into Geant4 primary vertex objects for use by the simulation. Each generator tool updates the HepMC objects based on the output information of the corresponding physics generator.

This design allows flexible integration of any physics generator of interest, via two principal methods:

- A standalone physics generator produces output data files in disks or buffers first, then the corresponding generator tool reads them and converts the format provided into HepMC objects.
- A physics generator is re-implemented as a generator tool which directly produces HepMC objects.

The particle gun *GenTool* generates particles with dedicated particle types, momenta and positions. The particle type can be specified with a PDG integer code, a particle name string, or an input file path. Particle name strings are parsed into PDG codes using `ROOT TDatabasePDG`. Using an input file provides an interface to generation of radioactive isotope decays using the Geant4 Radioactivity Decay Module (GRDM). The input file format specifies multiple radioactive isotopes with each line providing PDG code, mass, ratio and ranges of atomic number (Z) and mass number (A). During the particle generation the particle type is randomly sampled according to the ratio of each specified isotope. Limiting the ranges of Z/A for each radioactive isotope, allows a subset of the decay chain to be simulated.

The HepEvt *GenTool* converts events from HepEvt format to the HepMC format. A physics generator can be executed in advance of the simulation job and generate an output file with the HepEvt format, then the HepEvt *GenTool* reads events from the generated output file and performs the conversion to HepMC. Alternatively, the physics generator can be executed with `popen` using a Unix pipeline to avoid the need for intermediate files.

The GENIE *GenTool* uses another generator integration strategy, where the GENIE [29] libraries are linked to the simulation software and its functions are invoked from the GENIE *GenTool*. The GENIE output in GHEP data format is converted to the HepMC data format. The parameters needed to configure GENIE are set as properties of the GENIE *GenTool* that can be set from the user's Python scripts.

The position *GenTool* facilitates event generation either at fixed positions or uniformly distributed throughout a volume. Positions can be specified within named detector volumes or materials. Separation of this access to detector geometry information prevents duplication within other gentools. During the initialization of this tool, a recursive traversal of the Geant4 geometry is performed which caches transformation matrices for the volumes. When generating a position, a volume is selected according to the user specified volume name, then a bounding box is calculated by the Geant4 solid. Positions inside the bounding box are generated randomly and only the positions inside the solid are selected. Then the relevant cached transform is applied to obtain global positions from the generated local positions. In addition, global position cuts may be applied to limit the generated positions, such as restricting to a shell within a radius cut, or generating

positions within a layer using cuts along different axes. Subsequently, the Geant4 G4Navigator is used to access the material at this global position, allowing comparison with the user-specified material. The sampling is repeated until the user's requirements are fulfilled.

The time GenTool is used to control the timestamp of interaction vertices for each event and maintain the time correlation among vertices. In most cases, the timestamp of an event starts as zero in the detector simulation and is re-assigned in the electronics simulation. However, there are some exceptions, such as the supernova burst events, in which the timestamp is defined by the generator and used directly in the subsequent electronics simulation.

One challenge as mentioned previously is the handling of the dynamic deployment of the calibration sources. In order to generate particles from these calibration units from various positions without requiring multiple geometries, the units are implemented as detector elements, which can be placed into the containing detector element dynamically. The position GenTool traverses the Geant4 geometry to find calibration units by name and material. Subsequently, positions are sampled uniformly within the local volume and then transformed into global positions.

5 Detector simulation

5.1 Integration of Geant4 with JUNO simulation

Both SNIPEr and Geant4 have their own event loop control. A general simulation framework has been developed to adapt Geant4's event processing workflow into SNIPEr. The integration strategy of Geant4 and SNIPEr is illustrated in Fig. 4. The simulation framework comprises algorithms and services that adapt the original Geant4 workflow, acting as a bridge to provide flexible control of the underlying simulation. This approach allows most of the code from a standalone use of Geant4 to be used unchanged within the integration.

As shown on the right of Fig. 4, the simulation framework consists of four parts: an algorithm named DetSimAlg, which is the entrance to detector simulation; an implementation of a customized run manager named G4SvcRunManager, which is inherited from the G4RunManager in Geant4 toolkit to allow simulation of a single event; a service named IG4Svc, which controls the run manager; a service named IDetSimFactory, which is a factory to create instances of detector construction, physics list, primary generator and user actions. The simulation workflow is fully controlled with these components. At the initialization stage, DetSimAlg invokes instances of IG4Svc and IDetSimFactory to create the customized run manager which allows the Geant4 kernel to be initialized. At the execution of the event loop, DetSimAlg invokes the

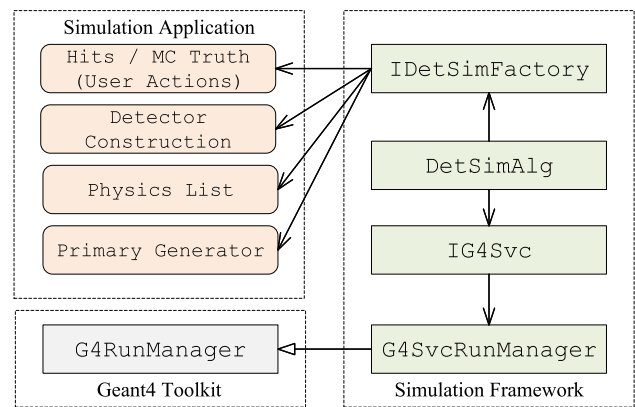


Fig. 4 Integration of Geant4 toolkit with JUNO simulation

run manager to simulate an event. In addition to the normal event loop, starting the Geant4 UI manager for visualization is also supported when users specify the `-vis` command line option.

As shown on the left of Fig. 4, a Geant4 simulation application consists of several parts: a detector construction to initialize the geometry; a physics list to initialize the particles and physics processes; a primary generator action to generate particles; user actions to handle detector response in sensitive detectors and other MC truth information. Some aspects of the simulation application can be customized using several SNIPEr tools. For detector construction, a detector element named `IDetElement` is used to represent a high-level detector component and manage the corresponding logical volumes in Geant4. The placements of one detector element into another detector element are handled with `IDetElementPos`, which returns the positions. Users can enable, disable, or modify the detector geometry easily, fulfilling requirements such as placing a calibration unit at a fixed position, changing the arrangement of PMTs, or disabling some detector components. Modular physics constructors, provided in Geant4, are used to build the physics list in the JUNO simulation. Each modular physics constructor is managed by a SNIPEr tool to support the configuration of parameters used in physics processes and models. This provides a flexible way for users to choose the proper physics models and parameters based on their requirements.

Geant4 user actions such as `UserSteppingAction` provide single entry points to access Monte Carlo truth information. However different analyses require access to different aspects of the truth information, presenting an organizational problem. This issue is solved by defining an `IAnalysisElement` interface which allows a user-configurable list of analysis elements to be composed where all have access to the MC truth information. The selection of truth information is stored within the Geant4 user track

information, which is retrieved at the end of the event and stored in output files.

5.2 Parameter management

The simulation software requires a large number of parameters to define the geometry of the detector and the optical properties of the materials and surfaces, physics processes, and characteristics of the electronics. Dedicated parameter access services have been implemented to provide consistent access to parameters from various applications and to facilitate flexible parameter variation during Monte Carlo tuning.

Examples of the optical properties of materials provided by the parameter service are refractive indices, absorption and scattering lengths, scintillator light yield, Birks constants, emission spectra, and time constants. Many of the parameters are energy dependent. The parameter service uses keys such as `Material.LS.RINDEX` to control the parameters to retrieve. Command line configuration allows default parameter values to be overridden.

Measurements of PMT parameters including quantum efficiency, collection efficiency, time spread, dark counting rate, gain, and resolution are stored in ROOT files with entries for every PMT. A dedicated PMT parameter service is implemented to provide access to these values to both the detector and electronics simulations using PMT identifier integers to select the PMT.

The parameters used in the simulation can be divided into static parameters which vary only infrequently with software updates and conditions data which change during data taking and require periodic calibrations with associated time ranges. Figure 5 illustrates how static parameters (in blue) and condition parameters (in green) with associated time intervals are grouped together with a `GlobalTag` that labels coherent parameter sets. For official data production, each offline software version will have one `GlobalTag` identifying the parameter set. The parameter services use a database interface to retrieve metadata that enables the parameters associated with the `GlobalTag` to be retrieved from the production file system. For MC tuning or user testing, it is possible to override the parameter files used.

The detector simulation, electronics simulation, and reconstruction algorithms handle the conditions data and parameter management in the same way.

5.3 Geometry construction

Flexible geometry management is particularly beneficial during detector design and optimization studies. The primary technique used to maintain a flexible geometry is to factorize the geometry into groups of volumes using the `IDetElement` base class and to mediate the composition of

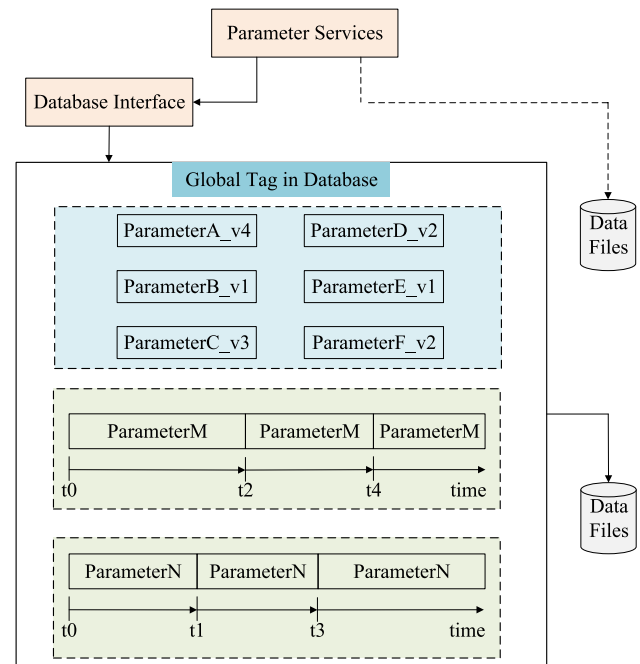


Fig. 5 Parameter management in simulation software. The versions of static parameters (in blue) and the time intervals of condition parameters (in green) are saved as `GlobalTag` in database

those detector elements using `inject` methods designed to retain independence between the detector elements. Figure 6 illustrates the usage of these detector elements. For example, the central detector is a detector element which directly contains only the liquid scintillator, its container, and the buffer material. The PMTs are not directly placed within the central detector, but their placement is mediated using the `IDetElement` instead. This simplifies interchanging different options for the central detector while keeping the arrangement of PMTs unchanged. This independence of the target geometry from the PMTs also proved useful for investigations of different types of PMTs.

Detector components and materials can be defined directly in Geant4 code or indirectly via parsing GDML (Geometry Description Markup Language) files or text files. Simulation of the calibration geometry elements, such as movable radioactive sources, uses a separate runtime geometry placement system.

The geometries of CD, WP, TT, calibration units, and other supporting structures in the JUNO detector have all been implemented in the simulation software according to the final design. As shown in Fig. 7, the simulated JUNO detector includes 3 layers of top tracker (red), 2400 WP PMTs (pink), 590 acrylic nodes (yellow), stainless steel truss (green), and chimney (blue). The 17612 20-in. PMTs and 25600 3-in. PMTs in the CD, calibration anchors inside and outside the acrylic sphere, and guide tube have also been implemented

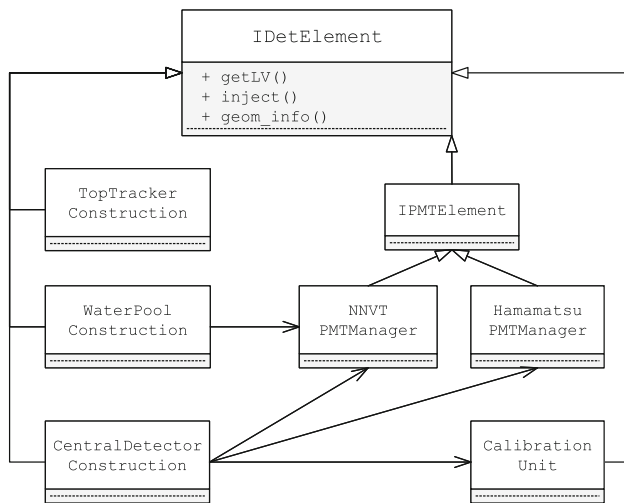


Fig. 6 Design and use of IDetElement detector elements

in the simulation software but not displayed in this figure in order to display other parts more clearly.

As shown in Fig. 8, in the central detector, two types of 20-in. PMTs are implemented in the detector simulation, including dynode-PMT produced by Hamamatsu and MCP-PMT manufactured by NNVT. Besides the PMT glass and inner vacuum, the PMT inner components, acrylic protection cover at the front, and steel protection cover at the back are also implemented. PMT inner components include a cylindrical tube at the bottom, a focusing electrode on the top, and a dynode (MCP) in the center of the focusing electrode. It is found that containing the PMT and protective cover within a virtual volume speeds up the Geant4 geometry initialization, presumably due to the complicated structure and large number of PMTs. The actual installation mounts PMTs into apertures through an optical mask used for optical isolation between the outer water pool and CD. To implement the optical mask geometry and account for the reflectivity of the mask in the simulation whilst avoiding expensive boolean geometry the tail of the 20-in. PMT is shortened to avoid overlap between the PMTs and optical mask. As optical effects arising from the tail of the PMT on the other side of the mask are expected to be negligible the PMT tails are not simulated. The detector geometry is defined using the Geant4 geometry model, while reconstruction, event display, and analysis packages are heavily dependent on ROOT. To provide a consistent detector description for different applications the GDML is chosen as the basis of the geometry management system [24]. Detector simulation reads geometry parameters from text files that are used to construct the geometry using the Geant4 C++ geometry model API. The complete geometry is exported using the Geant4 GDML writer into GDML files that serve as input to the geometry service using ROOT GDML import functionality. The ROOT geometry

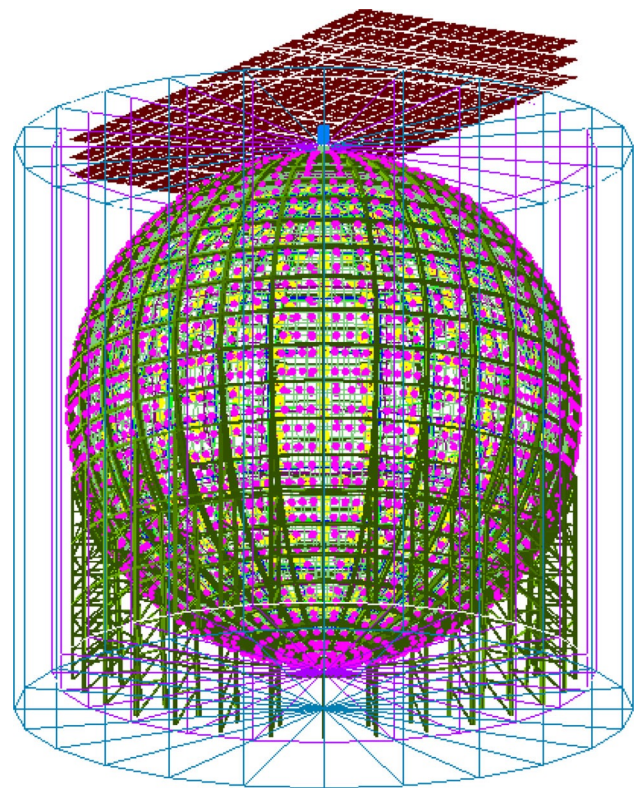


Fig. 7 JUNO detector in simulation software. 3 layers of top tracker (red), 2400 WP PMTs (pink), 590 acrylic nodes (yellow), stainless steel truss (green) and chimney (blue)

objects resulting from the import are used by the geometry service to construct mappings between detector identifiers and corresponding objects. The geometry service provides a detector information interface that is used by other applications including reconstruction, event display, and analysis. The consistency of the detector description relies on Geant4 GDML export and ROOT GDML import functionality.

5.4 Physics processes

Geant4 provides a set of physics constructors that are combined to build reference physics lists. Physics processes for JUNO detector simulation are created with the Geant4 physics constructors shown in Table 1. A Positronium process has been registered into the Livermore physics models G4EmLivermorePhysics. A modified neutron capture process has been registered in G4HadronPhysicsQGSP_BERT_HP.

The Geant4 Radioactivity Decay Module (GRDM) has been used for JUNO background evaluation. The correct treatment of ^9Li and ^8He decays is of fundamental importance in the study of cosmogenic backgrounds for JUNO. In GEANT4, the cosmogenic nuclei undergo beta decay of ^9Li and ^8He reaching the correct state. However, for the de-

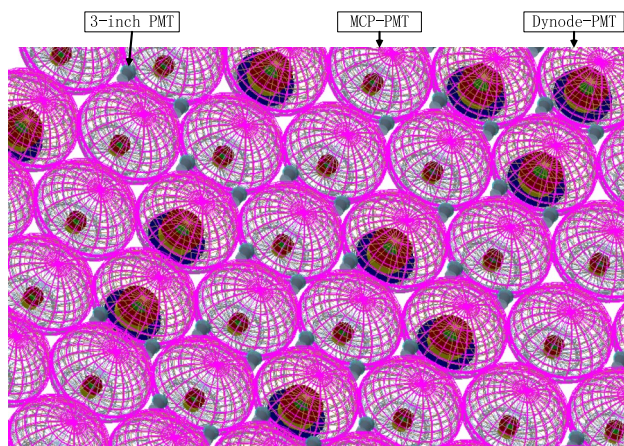


Fig. 8 Two types of 20-in. PMTs in CD, including dynode-PMT and MCP-PMT indicated with labels. The 20-in. dynode-PMTs have much larger electrodes inside the PMTs, compared with the MCP structures in the MCP-PMTs. The 3-in. PMTs are represented as the grey color and located in the gaps among 20-in. PMTs, in which only about 85% of gaps are filled with 3-in. PMTs. The acrylic protection cover is shown in mesh mode with a magenta color

Table 1 Geant4 Physics constructors used by JUNO simulation

Physics constructors	Status
G4EmLivermorePhysics	Customized
G4EmExtraPhysics	Unchanged
G4DecayPhysics	Unchanged
G4RadioactiveDecayPhysics	Customized
G4HadronPhysicsQGSP_BERT_HP	Customized
G4StoppingPhysics	Unchanged
G4IonPhysics or G4IonPhysicsPHP	Unchanged
G4OpticalPhysics	Customized

excitation of the ^9Be and ^8Li nuclei, the correct decay chains including alphas and neutrons are not accounted for. Thus the GRDM and the related data files have been modified to correctly handle ^9Li and ^8He decays, as described in [30]. Such a modification is now included in Geant4 since release 10.6.

For Ion processes, G4IonPhysics or G4IonPhysicsPHP can be chosen by users, depending on the particles to be simulated and the memory resources available. G4IonPhysicsPHP provides more reasonable simulation for the light nuclei at the MeV energy region, in which the G4TENDL data set is used. The TENDL cross-section table was substituted with that calculated by TALYS [31].

Geant4 processes that model optical photon propagation are G4OpBoundaryProcess, G4OpRayleigh and G4OpAbsorption, and are used by JUNO simulation. These processes use material properties such as refractive indices, absorption and scattering lengths and optical surface properties such as reflectivity which are set according

to measurements. The Geant4 processes that produce optical photons are G4Scintillation and G4Cerenkov. They were both modified to meet the needs of JUNO simulation. G4Cerenkov assumes a refractive index that monotonically increases with photon energy. As this is not the case for the JUNO LS refractive index the G4Cerenkov process was customized to handle more general refractive index characteristics. The G4Scintillation process was customized in several ways:

1. Different Birks constants were set for different particles.
2. Particle specific emission time constants and exponential decay components were used for gammas, electrons, positrons, alphas, neutrons and protons.
3. Photon reemission was implemented for the liquid scintillator, as optical photons arising from both scintillation and Cerenkov processes can be absorbed in the liquid scintillator and then re-emitted with a different wavelength. The reemission probability depends on wavelength.

Several physics constructors have been defined as SNIPEr Tools to facilitate flexible control and customization. For example users can easily switch on/off the scintillation or Cerenkov processes or customize properties of each process.

5.5 JUNO PMT optical model

The JUNO PMT optical model [32] accounts for both light interactions with the PMT window and optical processes inside the PMTs. The PMT optical model describes the angular and spectral response of the photon detection efficiency. A newly developed package uses the transfer matrix method (TMM) from optics to account for interference effects within the thin layers of anti-reflection coating and photocathode between the PMT glass and interior vacuum. Using inputs of layer thicknesses and complex refractive indices the TMM calculation yields reflectance, transmittance, and absorption of the multilayer stack of layers.

The JUNO PMT optical model is implemented as a Geant4 fast simulation model to integrate with the rest of the simulation. The fast simulation model is triggered only for optical photons within an envelope inside the PMT glass.

5.6 Hit persistency

After the simulation of PMT response, hits are created and registered into Geant4 hit collections. At the end of each event, the Geant4 hits are converted into the JUNO event data model (EDM) SimHits and saved into ROOT files. The EDM and ROOT I/O are described in Sect. 7.

For low energy events with energy deposit of 1 MeV the number of hits is less than 2000, with acceptable memory consumption of 800 MB with G4IonPhysics or 1.6 GB

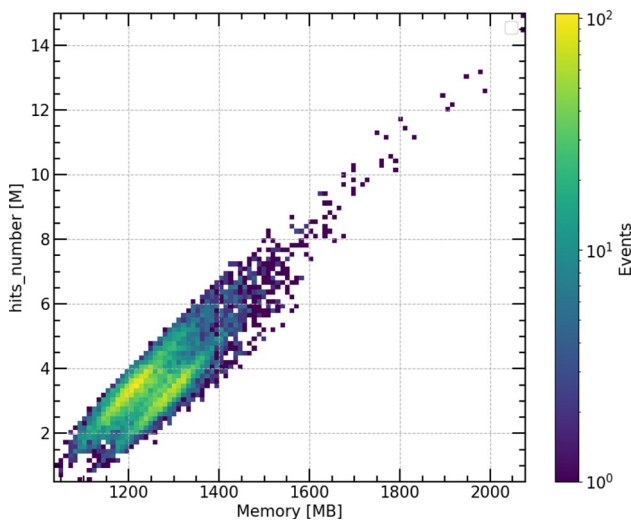


Fig. 9 Memory consumption versus number of hits in muon simulation

more with G4IonPhysicsPHP. The more memory consumption with the higher precision model arises from additional datasets that are loaded into memory.

High energy events, such as muons crossing the CD, can yield millions of simulated hits with memory consumption of up to 20 GB which poses operational difficulties. Several strategies have been developed to reduce this memory consumption.

1. Use smaller summary hits for high energy events that are about 20% the size of full hits and which contain only vital information such as arrival time and the number of photo-electrons.
2. Merge hits that arrive within a configurable time window. Using 1 ns to match the 1 GHz waveform sampling of the readout electronics reduces the number of hits to about 30% of the original for a muon of typical energy 215 GeV crossing the central detector.
3. Split processing of events that exceed configurable memory limits into sub-events. The sub-events are merged within the electronics simulation with sequential reads. ROOT writing is found to consume extra memory whilst simultaneously holding uncompressed and compressed buffers.

Without split processing, the maximum memory consumption for muon events can still exceed 6 GB. With splitting this maximum is reduced to about 2 GB for 14 million hits, when using G4IonPhysics, as shown in Fig. 9. This level of memory consumption fits within available computing resources allowing large scale production of simulation samples.

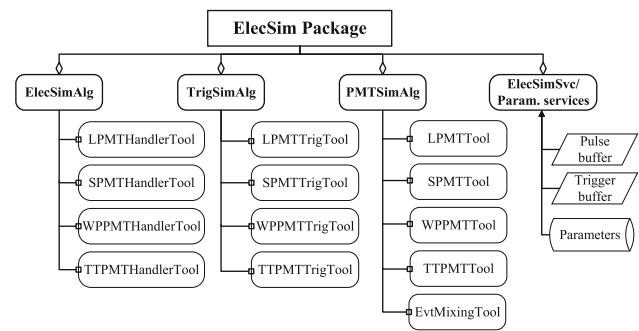


Fig. 10 Structure of the electronics simulation software

6 Event mixing and electronics simulation (ElecSim)

6.1 Electronics simulation software package

Package `ElecSim` is used to model the PMT response to hits from the Geant4-based `DetSim` package and also to model the readout electronics of CD, WP and TT using an implementation based on `SNiPER` managed dynamically loadable elements (DLE). The package incorporates an event mixing implementation that combines different event types to create simulated MC data that mimics real experimental data. Event mixing uses a “pull” based workflow (see 6.2) using `SNiPER` incident triggers that stays within reasonable memory budgets. `ElecSim` outputs become inputs to the online event classification algorithms (OEC) used for event tagging and may be saved to files using EDM formats and ROOT I/O services. Detailed descriptions of the JUNO PMT and electronics systems are available in prior publications [2, 33–35].

The components of the package are illustrated in Fig. 10, consisting of several services and three algorithms `PMTSimAlg`, `ElecSimAlg` and `TrigSimAlg`. The services manage the temporary Pulse and Trigger buffers which provide communication between the algorithms and also provide parameter access. The algorithms handle event mixing, PMT response modeling, electronics response modeling, and trigger response modeling. Each algorithm is implemented using four tools dedicated to each sub-system: LPM and SPMT systems in CD, the WP system, and the TT system.

The `EvtMixingTool` invoked by `PMTSimAlg` combines different types of physical events based on event rate inputs. Each physical event loaded is assigned a timestamp which allows the detector simulation hit time information to be adjusted prior to mixing. Subsequently, the hits are unpacked from the loaded events and converted into pulses

by the appropriate PMT tools, taking into account PMT effects such as gain resolution and variation, dark noise, pre-pulse and after-pulse, transit time, and transit time spread. Finally, all generated pulses are pushed into the pulse buffer in time order. This hit-level event mixing approach corresponds closely to the real-world situation, allowing the pileup of multiple event types to be handled naturally and correctly.

The `TrigSimAlg` sub-system tools simulate the actions of the corresponding hardware trigger cards. Simulated triggers are modelled by generating a trigger signal that is pushed into the trigger buffer together with trigger information. The tools used in `ElecSimAlg` sub-system process the pulses within the readout time window, applying various electronics effects such as waveform modelling and digitization and generating the outputs. Subsequently, EDM objects are created and filled by corresponding handler tools.

6.2 “Pull” mode workflow

As physical events may produce multiple readout events spanning hundreds of microseconds, or even longer, event mixing implementations must carefully manage memory resources. The “pull” mode avoids excessive memory usage with user configurable time ranges and a processing time window (PTW) which is longer than the readout time window. Only events within the PTW are loaded, unpacked and mixed.

In reality, PMT hits are triggered leading to pulses that are digitized into readout events. Pull mode mixing, as illustrated in Fig. 11, operates in the reverse manner starting from `ElecSimAlg`, which creates readout events only when a trigger can be created from the simulated pulses. When the trigger buffer is empty `TrigSimAlg` looks for pulses to create a trigger. If there are insufficient pulses within the PTW to produce a trigger, the pulses within and before the PTW are deleted and a new PTW is opened and populated with pulses by the `PMTSimAlg` loading more events with timestamps inside the PTW. The `TrigSimAlg` continues to try to create a trigger from the updating pulse buffer until it succeeds allowing `ElecSimAlg` to create a readout event. Both pulse and trigger buffers operate in pipeline style with processed data removed and new data added.

The implementation is organized using `SNiPER` roles, each algorithm is associated with a task that is only invoked when there is insufficient data in the corresponding buffer. Communication between the algorithm and task uses the `SNiPER` incident mechanism. When a task is invoked, registered algorithms and tools are executed once and tools registered in the algorithm are also invoked. This leads to all the relevant services of the tasks being updated.

To mix events from different files, users need only assign labels and rates to the event types. The mixing implemen-

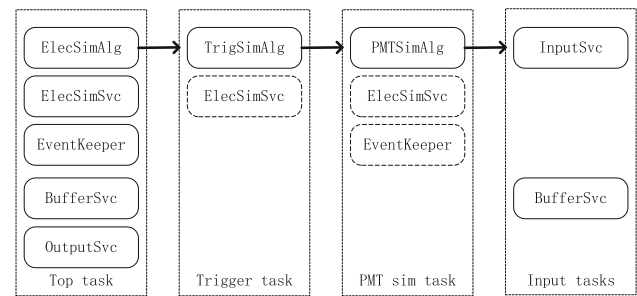


Fig. 11 Pull mode electronics simulation workflow showing objects relevant to each task with dashed boxes indicating shared objects. The arrows illustrate the control hierarchy between the tasks with `ElecSimAlg` from the top task invoking `TrigSimAlg` when the trigger buffer is empty. `TrigSimAlg` in turn invokes `PMTSimAlg` when the pulse buffer has insufficient pulses, which in turn invokes `InputSvc` to load the various event types

tation then proceeds as described above, writing events that mimic real data into the output buffer.

7 Data model, MC truth and event correlation

7.1 Event data model and ROOT I/O

The JUNO event data model (EDM) [23] defines the content of the event data objects consumed and produced by all the algorithms that constitute the simulation workflow, as shown in Table 2. The physics generator algorithm produces `GenEvt` objects that are consumed by the detector simulation algorithm in order to produce `SimEvt` objects. Finally, the electronics simulation consumes `SimEvt` objects and produces `TriggerEvt` and `ElecEvt` objects.

All event data objects follow a two-level design with lightweight header objects that refer to event objects containing the bulk of the data. An event navigator consists of a list of header objects, which can be accessed by the corresponding EDM path. The header objects are loaded into memory first, subsequently, event objects are loaded only when needed reducing resource usage.

The output of detector simulation stores both `GenEvt` and `SimEvt`. `GenEvt` objects refer to `HepMC::GenEvent`. ROOT dictionaries of `HepMC` objects are generated to facilitate access when persisted to ROOT files. `SimEvt` objects hold collections of tracks, and hits in CD, WP and TT. The track class includes members such as particle type, positions, momenta and total deposited energy. Both primary and secondary tracks from `Geant4` are stored. Storage of secondaries is especially relevant with the neutron capture process and radioactivity decay processes. Hits from the CD and WP share a common hit type, with a separate type used for TT hits.

Table 2 Event data models used by JUNO simulation

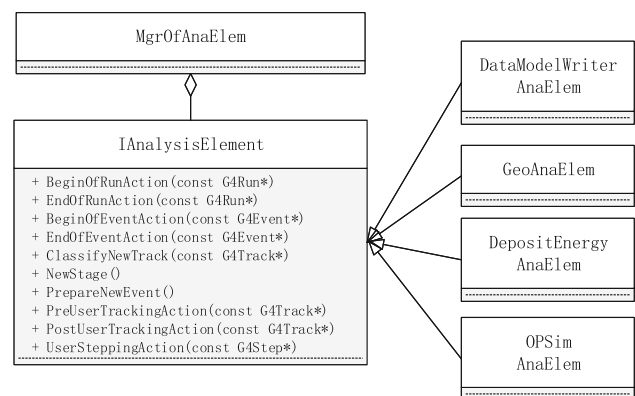
Stage	Header object	Event object	Contained objects	Default EDM path
Generator	GenHeader	GenEvt	Tracks	/Event/Gen
Simulation	SimHeader	SimEvt	Tracks and hits (CD/TT/WP)	/Event/Sim
Trigger	CdTriggerHeader	CdTriggerEvt		/Event/CdTrigger
	WpTriggerHeader	WpTriggerEvt		/Event/WpTrigger
	TtTriggerHeader	TtTriggerEvt		/Event/TtTrigger
Readout	CdWaveformHeader	CdWaveformEvt	Waveforms (CD)	/Event/CdWaveform
	CdLpmtElecHeader	CdLpmtElecEvt	t/q pairs (CD LPMT)	/Event/CdLpmtElec
	CdSpmtElecHeader	CdSpmtElecEvt	t/q pairs (CD SPMT)	/Event/CdSpmtElec
	WpElecHeader	WpElecEvt	t/q pairs (WP)	/Event/WpElec
	WpWaveformHeader	WpWaveformEvt	Waveforms (WP)	/Event/WpWaveform
	TtElecHeader	TtElecEvt	t/q pairs (TT)	/Event/TtElec

The outputs from the electronics simulation consist of triggers and readouts. The trigger types are divided into three classes: CdTriggerEvt, WpTriggerEvt and TtTriggerEvt. The readout types are divided into six classes: CdWaveformEvt stores the waveforms of LPMTs in CD; CdLpmtElecEvt stores time and charge pairs of LPMTs in CD; CdSpmtElecEvt stores time and charge pairs of SPMTs in CD; WpElecEvt stores time and charge pairs in WP; WpWaveformEvt stores the waveforms in WP; TtElecEvt with time and charge pairs in TT. This design provides flexibility to match resource usage to requirements.

A ROOT-based I/O system is used to read and write event data model objects. On reading an event from a file the input service first reads an event navigator object. Loading of header and event objects is deferred until requested, avoiding unnecessary I/O. When writing an event the output service writes the event navigator, header objects, and event objects. Only headers and event objects associated with the event navigator are written.

In order to reduce memory usage in the detector simulation, a huge event is split into sub-events. All the information except the collection of PMT hits in CD are stored in the first sub-event, while the collection of PMT hits in the CD are split into the rest sub-events. The event navigators share the same information for these sub-events. Using a dedicated ROOT input service, these sub-events could be merged again according to the same information from event navigators. Such features are configured with separate SNIPEr sub-tasks that are invoked using an incident mechanism.

The loading of various event samples needed for event mixing is implemented using the SNIPEr multiple sub-tasks feature. Each sub-task is configured with an input service and a buffer management service. When event mixing loads a sample the corresponding sub-task is invoked causing the

**Fig. 12** Geant4 user action access from multiple independent tools

input service to load the event into the data buffer providing access to the corresponding input task.

7.2 Monte Carlo truth

Geant4 user actions provide access to MC truth information via objects such as G4Event, G4Track, and G4Step. This access is shared with multiple independent tools, as illustrated in Fig. 12, using a tool manager that maintains a list of tools that implement the IAnalysisElement interface. The Geant4 user actions via the tool manager invoke the corresponding methods of all the tools according to their registration order.

7.3 Event correlation

Events at the physics event level, such as from the IBD process, may be split into two or more events at the readout event level and also background events may be mixed in with signal events. Figure 13 shows how to handle such

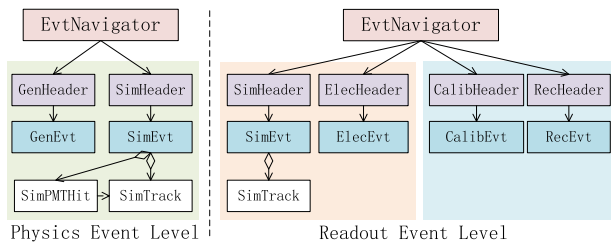


Fig. 13 Event correlation handling

a case. An *EvtNavigator* object that maintains references to associated objects allows the relationships between objects at different levels to be navigated, for example, relating readout objects at the electronics simulation level with primary particles at the detector simulation level. When a detector simulation event is split into two readout objects, two *EvtNavigator* objects at readout event level will be created and both maintain information concerning the primary stage, so the events after reconstruction could be correlated with the same *SimTrack* objects. An *EventKeeper* utility is provided that, using the relationship information recorded in the *EvtNavigator* objects, is able to rebuild *SimEvt* corresponding to readout events including all the track level information. The number of hits contributing to the readout is also provided, but hit objects are not duplicated.

8 Strategies to improve computing performance

8.1 Multi-threaded detector simulation

JUNO simulation has been updated to enable multi-threaded running, profiting from Geant4 functionality that provides event-level parallelization. Events are processed in different threads, while the detector geometry is shared. For the JUNO geometry with many thousands of PMTs, this enables a significant reduction in memory resources. The parallelized SNiPER framework is implemented using high-level task objects provided by the Intel Threading Building Blocks (TBB) library, avoiding low-level thread management. Each task object is configured with *Algorithm* and *Service* components and then scheduled to run in a dedicated thread.

Parallelized processing presents a challenge in handling events which must retain their time ordering, such as events from a supernova burst. A global buffer-based technique is developed [36] to maintain time ordering, that orders generated objects within the global buffer prior to simulating each in dedicated threads. Finally completed events are saved by a ROOT I/O service from another dedicated thread [37].

8.2 Fast simulation

The huge computational and memory demands of the full JUNO simulation of millions of optical photons has moti-

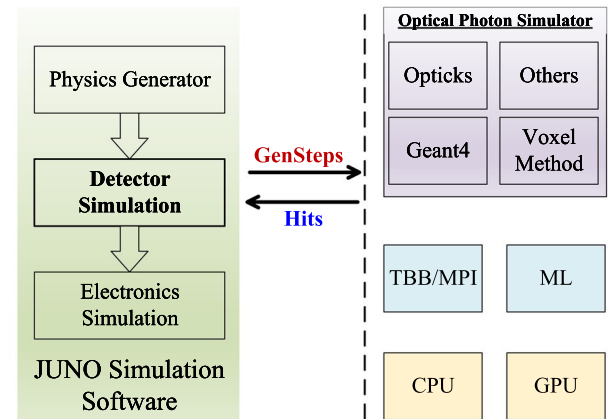


Fig. 14 Deferred optical propagation method to integrate different optical photon simulators

vated the development of a voxel-based parameterization [38]. Instead of propagating optical photons the parameterization samples pre-generated distributions of the number of photoelectrons and hit times representing the PMT response. At each step the appropriate distributions for the current position is accessed allowing random sampling to yield a number of photoelectrons and hit time for each PMT.

Figure 14 illustrates a unified approach to integrating the various optical photons simulators which allow the optical simulation to be deferred until after selection criteria have been satisfied [39]. The simulators include the standard Geant4 optical photon simulator, the voxel method and the Opticks GPU-based simulator.

8.3 Opticks GPU optical photon simulation

Opticks [22,40] performs a full optical photon simulation equivalent to the Geant4 optical photon simulation that benefits from the high performance ray tracing provided by NVIDIA GPUs. The Opticks implementation is based on the NVIDIA OptiX 7 API [41]. All aspects of the Geant4 context relevant to optical photon generation and propagation such as the detector geometry, optical physics and the optical photons are translated into appropriate forms and are uploaded to the GPU. Detector geometry on the GPU is modelled with NVIDIA OptiX intersection, bounding box and closest hit programs and the buffers that these programs access. Opticks provides an automated translation of Geant4 geometries into these buffers, starting by traversing the Geant4 volume tree converting materials, surfaces, solids, volumes and sensors into Opticks equivalents.

Photons are brought to the GPU via NVIDIA OptiX ray generation programs which contain CUDA ports of the photon generation loops from Geant4 scintillation and Cerenkov processes. These programs together with “Genstep” data

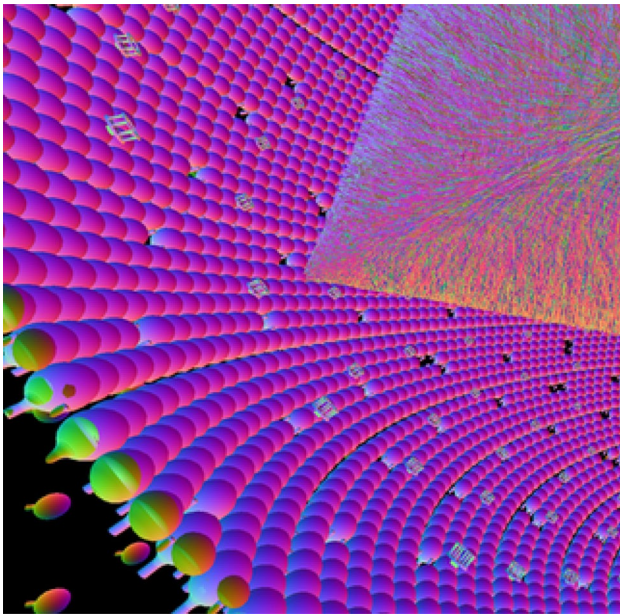


Fig. 15 This figure shows the Cerenkov and scintillation photons produced by a 200 GeV muon traveling across the JUNO detector. Each line represents a single optical photon and colors indicate the polarization direction. The gaps among PMTs are caused by the stainless steel supporting bars which are not shown in the picture. These bars are used to support the acrylic sphere

structures which are collected from Geant4 on the CPU allow the photons to be generated on the GPU. As Geant4 has no “Genstep” interface it is necessary to modify the classes representing scintillation and Cerenkov processes. Instead of generating photon secondary tracks in a loop the “Genstep” parameters such as the process type code, the number of photons to generate and the line segment along which to generate them and all other parameters used in the generation loop are collected and uploaded to the GPU, typically at the end of the event. This allows the photons to be allocated, generated and propagated entirely on the GPU, minimizing transfer overheads and allowing CPU memory usage to be restricted to optical photons that hit photomultiplier tubes, which are copied back to the CPU and added to Geant4 hit collections, allowing the rest of the simulation to proceed unmodified. As illustrated in Fig. 15 Opticks also provides OpenGL GPU based visualizations of detector geometries and optical photon propagations.

Offloading the computational and memory burdens of simulating millions of optical photons to the GPU eliminates processing bottlenecks. As the optical photons in JUNO can be considered to be produced only by the scintillation and Cerenkov processes and yield only hits on photomultiplier tubes it is straightforward to integrate the Opticks external optical photon simulation together with the Geant4 simulation of all other particles. Reference [22] provides further

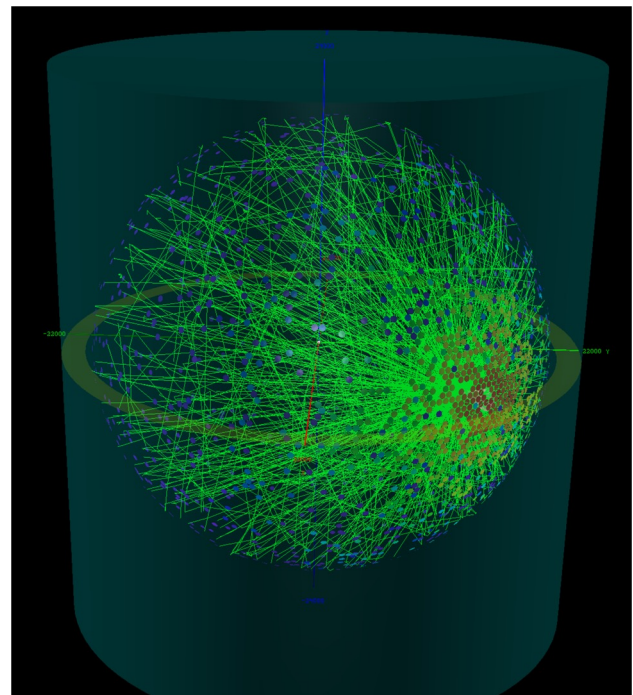


Fig. 16 SERENA display of particle trajectories in a simulated event

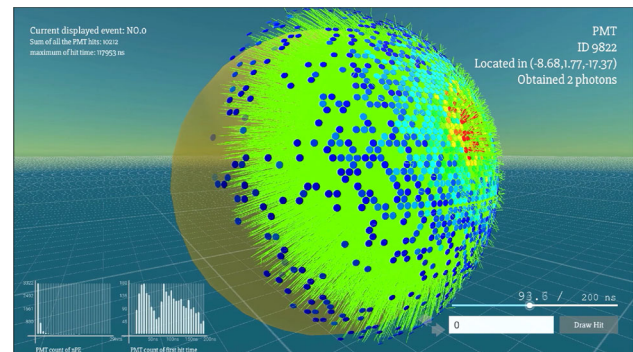


Fig. 17 ELAINA display of particle trajectories in a simulated event

details on Opticks and its integration with the JUNO simulation framework and potential performance benefits.

9 Visualization

Visualizations of detector geometries and of actual and simulated events provide the most effective way to communicate the principals of detector operation to students and the general public. Interactive display interfaces that present particle trajectories, physics processes and hits on detector elements can greatly assist understanding and prove insightful for the development of reconstruction and calibration approaches. In addition, visualization is vital for the development of the simulation allowing geometry problems such as overlaps to be identified.

SERENA [26] and ELAINA [27] are two independent event display applications developed for JUNO. SERENA is a ROOT based event display package that is integrated with the offline software geometry service [24, 42] and event data model. By reading the output files from the simulation program, the trajectories and hits in an MC event can be visualized in the event display package, as shown in Figs. 16 and 17. Users also have the flexibility to filter or highlight different physical processes or optical processes, such as Fresnel refraction, total internal reflection, or Rayleigh scattering. The interface allows the selection of specific trajectories or hits for which to display further information. The other event display application ELAINA is an Unity [43] based program which is independent of the offline software, facilitating installation on a wide range of operating systems and providing eye-catching visual effects.

10 Summary

Simulation software is an essential component of the JUNO experiment, playing an important role across detector design and commissioning, offline data processing and physics analysis. The simulation software must be well designed and implemented and operate with reasonable computing resources in order to meet the needs of the experiment throughout its life time of more than 30 years. The broad energy range of JUNO's physics program from keV to GeV, and the scale of the JUNO detector make it challenging to achieve this goal. This paper has presented the design and implementation of the JUNO simulation software, comprising the four building blocks of generator, detector simulation, event mixing and electronics simulation. The software is developed in C++ and Python and is based on the SNIPEr framework and depends on several external libraries, including Geant4, CLHEP, ROOT and BOOST. A modular design style has been used, based on SNIPEr dynamically loadable elements DLEs, enhancing maintainability, extensibility and reliability.

Key challenges of the simulation have been highlighted together with strategies to address them. A unified and flexible generator interface has been developed that facilitates the integration of diverse physics generators and dynamic deployment of calibration sources. Flexible parameter access from a variety of data sources, such as files and databases, is provided via a single consistent interface used from all processing stages.

Several approaches to improve the computing performance of high energy event simulation are implemented, for example reducing memory consumption with multi-threading, merging hits and event splitting or using a parameterized fast simulation. Integration with Opticks speeds up

the simulation and reduces CPU memory consumption by offloading the optical photon simulation to the GPU.

Time correlated experimental data is mimicked using hit-level event mixing implemented with a “pull” mode that limits memory consumption. Machinery that maintains object relationships despite splits and merges arising from the simulation and utilities giving complete Monte Carlo truth information for readout events are provided.

The JUNO simulation software has been successfully used to perform large scale Monte Carlo productions for the JUNO collaboration. Attaining the goal of providing a precise reproduction of experimental data across a broad range of physics analyses in JUNO requires a long-term commitment to ongoing development that strives to continually improve our understanding of the JUNO detector and the performance of the simulation.

Acknowledgements We gratefully acknowledge support from the Strategic Priority Research Program of the Chinese Academy of Sciences (CAS), Grant No. XDA10010900. This work is also supported in part by National Natural Science Foundation of China (NSFC) under grant No. 11875279, No. 12275293, and No. 12025502, supported in part by Youth Innovation Promotion Association, CAS. This work has been partially supported by CNPq, grant No.407149/2021-0.

Data Availability Statement This manuscript has no associated data or the data will not be deposited. [Authors' comment: The datasets generated during the current study are available from the corresponding author on reasonable request].

Open Access This article is licensed under a Creative Commons Attribution 4.0 International License, which permits use, sharing, adaptation, distribution and reproduction in any medium or format, as long as you give appropriate credit to the original author(s) and the source, provide a link to the Creative Commons licence, and indicate if changes were made. The images or other third party material in this article are included in the article's Creative Commons licence, unless indicated otherwise in a credit line to the material. If material is not included in the article's Creative Commons licence and your intended use is not permitted by statutory regulation or exceeds the permitted use, you will need to obtain permission directly from the copyright holder. To view a copy of this licence, visit <http://creativecommons.org/licenses/by/4.0/>.

Funded by SCOAP³. SCOAP³ supports the goals of the International Year of Basic Sciences for Sustainable Development.

References

1. F. An et al., J. Phys. G **43**(3), 030401 (2016). <https://doi.org/10.1088/0954-3899/43/3/030401>
2. Prog. Part. Nucl. Phys. **123**, 103927 (2022). <https://doi.org/10.1016/j.pnpnp.2021.103927>
3. Z. Djurcic, et al., (2015)
4. S. Agostinelli et al., Nucl. Instrum. Methods A **506**, 250 (2003). [https://doi.org/10.1016/S0168-9002\(03\)01368-8](https://doi.org/10.1016/S0168-9002(03)01368-8)
5. J. Allison et al., IEEE Trans. Nucl. Sci. **53**, 270 (2006). <https://doi.org/10.1109/TNS.2006.869826>
6. J. Allison et al., Nucl. Instrum. Methods A **835**, 186 (2016). <https://doi.org/10.1016/j.nima.2016.06.125>

7. J.H. Zou, X.T. Huang, W.D. Li, T. Lin, T. Li, K. Zhang, Z.Y. Deng, G.F. Cao, J. Phys. Conf. Ser. **664**(7), 072053 (2015). <https://doi.org/10.1088/1742-6596/664/7/072053>
8. <https://github.com/SNiPER-Framework>
9. X. Li, Z. Deng, L. Wen, W. Li, Z. You, C. Yu, Y. Zhang, T. Lin, Chin. Phys. C **40**(2), 026001 (2016). <https://doi.org/10.1088/1674-1137/40/2/026001>
10. A. Abusleme et al., JHEP **03**, 004 (2021). [https://doi.org/10.1007/JHEP03\(2021\)004](https://doi.org/10.1007/JHEP03(2021)004)
11. Z. Li et al., Nucl. Sci. Tech. **32**(5), 49 (2021). <https://doi.org/10.1007/s41365-021-00885-z>
12. Z. Qian et al., Nucl. Instrum. Methods A **1010**, 165527 (2021). <https://doi.org/10.1016/j.nima.2021.165527>
13. Z.Y. Li, Z. Qian, J.H. He, W. He, C.X. Wu, X.Y. Cai, Z.Y. You, Y.M. Zhang, W.M. Luo, Nucl. Sci. Tech. **33**(7), 93 (2022). <https://doi.org/10.1007/s41365-022-01078-y>
14. K. Zhang, M. He, W. Li, J. Xu (2018). <https://doi.org/10.1007/s41605-018-0040-8>
15. C.F. Yang, Y.B. Huang, J.L. Xu, D.R. Wu, H.Q. Lu, Y.P. Zhang, W.M. Luo, M. He, G.M. Chen, S.Y. Zhang, Nucl. Sci. Tech. **33**(5), 59 (2022). <https://doi.org/10.1007/s41365-022-01049-3>
16. A. Abusleme et al., JHEP **11**, 102 (2021). [https://doi.org/10.1007/JHEP11\(2021\)102](https://doi.org/10.1007/JHEP11(2021)102)
17. X. Huang, T. Li, J. Zou, T. Lin, W. Li, Z. Deng, G. Cao, PoS ICHEP2016, 1051 (2017). <https://doi.org/10.22323/1.282.1051>
18. L. Lonnblad, Comput. Phys. Commun. **84**, 307 (1994). [https://doi.org/10.1016/0010-4655\(94\)90217-8](https://doi.org/10.1016/0010-4655(94)90217-8)
19. <https://www.boost.org>
20. R. Brun, F. Rademakers, Nucl. Instrum. Methods A **389**, 81 (1997). [https://doi.org/10.1016/S0168-9002\(97\)00048-X](https://doi.org/10.1016/S0168-9002(97)00048-X)
21. <https://gitlab.cern.ch/gaudi/Gaudi>
22. S. Blyth, EPJ Web Conf. **251**, 03009 (2021). <https://doi.org/10.1051/epjconf/202125103009>
23. T. Li, X. Xia, X. Huang, J. Zou, W. Li, T. Lin, K. Zhang, Z. Deng, Chin. Phys. C **41**(6), 066201 (2017). <https://doi.org/10.1088/1674-1137/41/6/066201>
24. K. Li, Z. You, Y. Zhang, J. Zhu, T. Lin, Z. Deng, W. Li, Nucl. Instrum. Methods A **908**, 43 (2018). <https://doi.org/10.1016/j.nima.2018.08.008>
25. S. Zhang, J.S. Li, Y.J. Su, Y.M. Zhang, Z.Y. Li, Z.Y. You, Nucl. Sci. Tech. **32**(2), 21 (2021). <https://doi.org/10.1007/s41365-021-00852-8>
26. Z. You, K. Li, Y. Zhang, J. Zhu, T. Lin, W. Li, JINST **13**(02), T02002 (2018). <https://doi.org/10.1088/1748-0221/13/02/T02002>
27. J. Zhu, Z. You, Y. Zhang, Z. Li, S. Zhang, T. Lin, W. Li, JINST **14**(01), T01007 (2019). <https://doi.org/10.1088/1748-0221/14/01/T01007>
28. M. Dobbs, J.B. Hansen, Comput. Phys. Commun. **134**, 41 (2001). [https://doi.org/10.1016/S0010-4655\(00\)00189-2](https://doi.org/10.1016/S0010-4655(00)00189-2)
29. C. Andreopoulos et al., Nucl. Instrum. Methods A **614**, 87 (2010). <https://doi.org/10.1016/j.nima.2009.12.009>
30. C. Jollet, A. Mereaglia, Nucl. Instrum. Methods A **949**, 162904 (2020). <https://doi.org/10.1016/j.nima.2019.162904>
31. A.J. Koning, D. Rochman, J.C. Sublet, N. Dzysiuk, M. Fleming, S. van der Marck, Nucl. Data Sheets **155**, 1 (2019). <https://doi.org/10.1016/j.nds.2019.01.002>
32. Y. Wang, G. Cao, L. Wen, Y. Wang, Eur. Phys. J. C **82**(4), 329 (2022). <https://doi.org/10.1140/epjc/s10052-022-10288-y>
33. A. Abusleme et al., Eur. Phys. J. C **82**(12), 1168 (2022). <https://doi.org/10.1140/epjc/s10052-022-11002-8>
34. M. Bellato et al., Nucl. Instrum. Methods A **985**, 164600 (2021). <https://doi.org/10.1016/j.nima.2020.164600>
35. X. Fang, Y. Zhang, G.H. Gong, G.F. Cao, T. Lin, C.W. Yang, W.D. Li, JINST **15**(03), P03020 (2020). <https://doi.org/10.1088/1748-0221/15/03/P03020>
36. J. Zou, T. Lin, W. Li, X. Huang, Z. Deng, G. Cao, Z. You, EPJ Web Conf. **214**, 05026 (2019). <https://doi.org/10.1051/epjconf/201921405026>
37. T. Lin, J. Zou, W. Li, Z. Deng, G. Cao, X. Huang, Z. You, EPJ Web Conf. **214**, 02008 (2019). <https://doi.org/10.1051/epjconf/201921402008>
38. T. Lin, Z.Y. Deng, W.D. Li, G.F. Cao, Z.Y. You, X.Y. Li, Chin. Phys. C **40**(8), 086201 (2016). <https://doi.org/10.1088/1674-1137/40/8/086201>
39. T. Lin, J. Phys. Conf. Ser. **2438**(1), 012078 (2023). <https://doi.org/10.1088/1742-6596/2438/1/012078>
40. <https://bitbucket.org/simonciblyth/opticks/>
41. S.G. Parker, J. Bigler, A. Dietrich, H. Friedrich, J. Hoberock, D. Luebke, D. McAllister, M. McGuire, K. Morley, A. Robison, M. Stich, ACM Trans. Graph. **29**(4) (2010). <https://doi.org/10.1145/1778765.1778803>
42. K. Huang, Z. Li, Z. Qian, J. Zhu, H. Li, Y. Zhang, S. Sun, Z. You, Nucl. Sci. Tech. **33**(11), 142 (2022). <https://doi.org/10.1007/s41365-022-01133-8>
43. <http://unity.com>